PAPER REF: 4042

NUMERICAL MODELLING AND EXPERIMENTAL CHARACTERIZATION OF POMBALINO "FRONTAL" WALL CYCLIC BEHAVIOR

Ana Maria Gonçalves(*), João Gomes Ferreira [1], Luis Guerreiro[1], Fernando Branco[1]

[1]Instituto Superior Técnico, Lisboa, Portugal
(*)*Email:* goncalves.amn@gmail.com

ABSTRACT

After the large destruction of Lisbon due to the 1755 earthquake, the city had to be almost completely rebuilt. The innovative "pombaline" buildings were then developed. This type of building is characterized by its structural interior "frontal" walls in elevated floors, constituted by a timber frame with vertical and horizontal elements, braced with diagonal elements (Saint Andrew's crosses) with masonry infill.

This paper describes an experimental campaign to assess the in-plane cyclic behaviour of "frontal" walls and to evaluate the effect of its different components (timber frame, masonry). Experimental characterization of the in-plane behaviour was carried out by static cyclic shear testing with controlled displacements.

Along with the experimental characterization, the numerical modeling of the structural elements tested is developing using the ABAQUS software. Those models were calibrated based on the experimental structural element behavior and parametric studies were then conducted.

Keywords: "Pombaline" buildings, cyclic loading tests, earthquake, Abaqus This work

INTRODUCTION

The "pombaline" buildings, named after the Marquis of Pombal, in particular, present a structure with maximum of four storeys, with arcades at the ground floor, masonry facade walls and internal timber framed masonry walls. These walls, together with the floors' timber beams, form the 3-D cage that constitutes the seismic resistant structure. The Marquis of Pombal ordered their construction after the 1755 earthquake that destroyed Lisbon, aiming at providing the city with seismic resistant buildings (Ferreira, et al. 2012).

Though these structures have a good anti-seismic design, after more than 250 years the buildings need rehabilitation works because of their degradation, the inadequate interventions they have been subjected to (such as adding storeys, modifying structural elements or changing the functionality of the building) and because the new codes establish more demanding rules regarding earthquake resistance.

It was the limited knowledge on the whole behavior of the cage system, and particularly on timber framed wall's behavior, that motivated the experimental program presented in this paper.

EXPERIMENTAL PROGRAM

Objectives

The objective of the experimental work developed and presented herein is to obtain the cyclic behaviour of the timber framed walls through static cyclic shear testing under controlled displacements. Simple timber frames (without masonry infill) were also tested to assess the contribution of these frames to the overall behaviour of the timber-masonry wall.

Tested specimens

The tested specimens present four Saint Andrew's crosses each. Two models consist of the simple timber frames without masonry infill, referred to as "timber frames - TF". The other two specimens have identical timber frames but present masonry infill and are referred to as "masonry walls - MW" (Fig. 1).

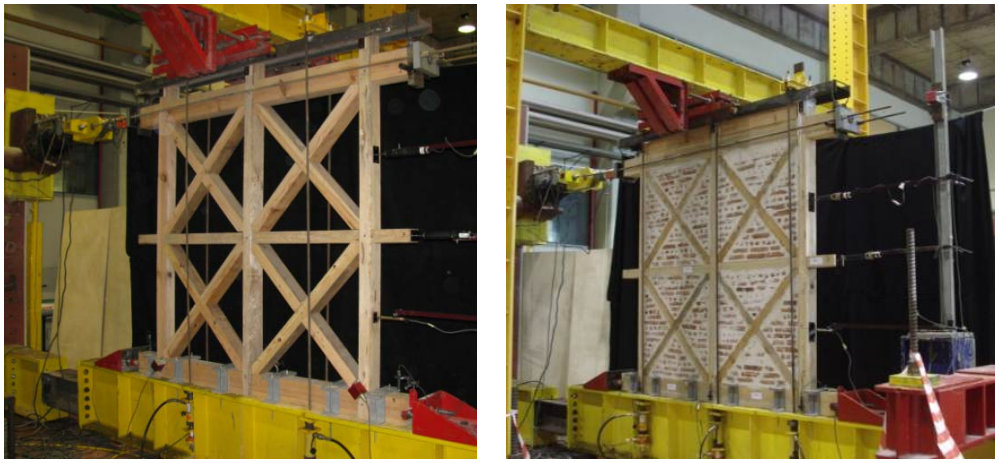

a)Timber frame (TF) specimen b) Masonry wall (MW) specimen

Fig.1 Tested specimens.

The characteristics of the walls constructions and the description of experimental procedures on test are present in Gonçalves et al (2012).

RESULTS

Timber Frames (TF)

The load-displacement diagrams obtained for the timber frames (TF) are shown in Fig. 2 The cyclic displacements were imposed until submitting the walls to rupture. An increase in the walls stiffness, occurring for displacement higher than about 60 mm, was identified in the load-displacement diagrams. However, this boost in the wall stiffness is due to the increase of strength in the tensioned cables jacks, when they reach their limit course and start to behave as tie rods. Due to this behaviour, these values cannot be taken into account for the characterization of the walls. The analysis is limited to a range of ± 55 mm displacements, which corresponds to a significant drift of 2.6%.

The hysteretic behaviour of the "frontal" walls subjected to cyclic loading is characterized by nonlinear behaviour with a high ductility response. The maxim strength is 30 kN for the timber frame walls, measured at the displacement of 55 mm (2.6% drift).

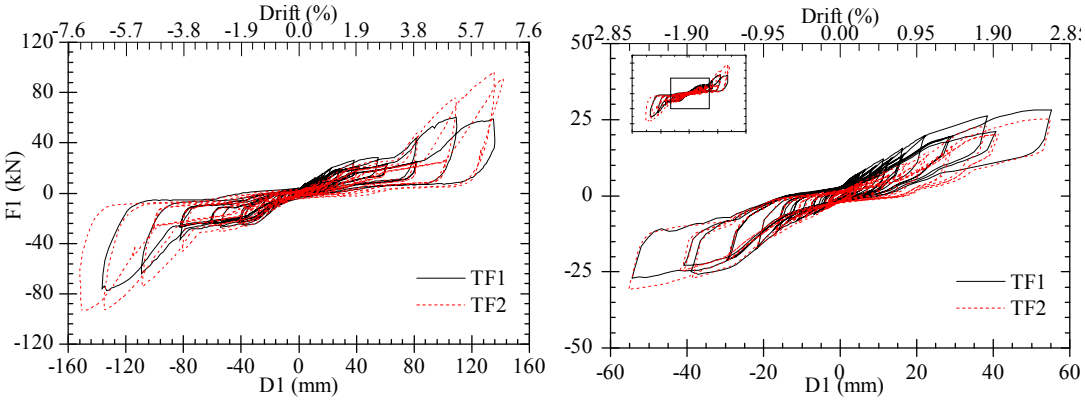

Fig.2 Force-Displacement curves of timber frames.

As shown in Fig.3, in the first cycles the timber frame walls present practically bilinear behaviour, up to approximately 12 mm (0.5% drift). As displacements increase, a number of effects such as cracking and plasticization or degradation of stiffness became more visible.

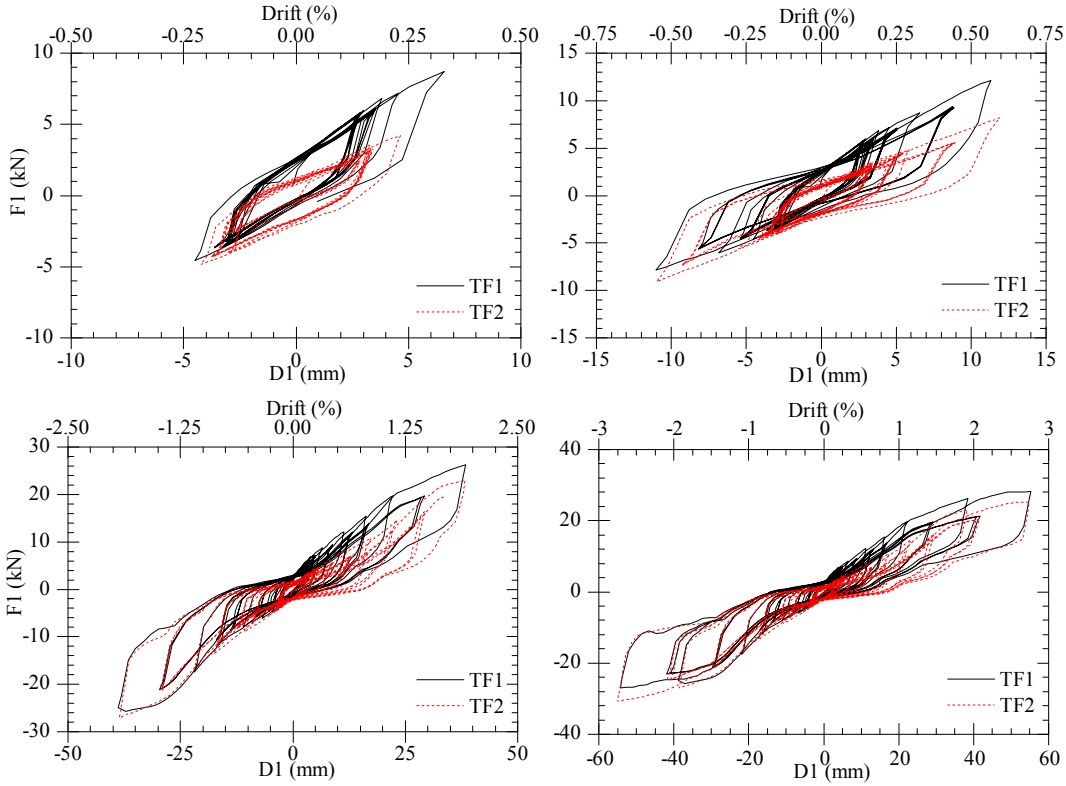

Fig.3 Force-displacement curves of timber frames along the displacement history.

The locus of extremities of the load-displacement hysteresis loops are envelope curves. The envelope curve contains the peak loads of the first cycle of each segment of the cyclic loading. Wall displacement in the positive direction produces a positive envelope curve; the negative wall displacement produces a negative envelope curve.

According to ISO 21581 (2009), the first, second and third envelope curves for the cyclic tests shall be established by connecting the points of maximum load in the hysteresis plot in each displacement level in the first, second and third reversed cycles, respectively (Fig. 4).

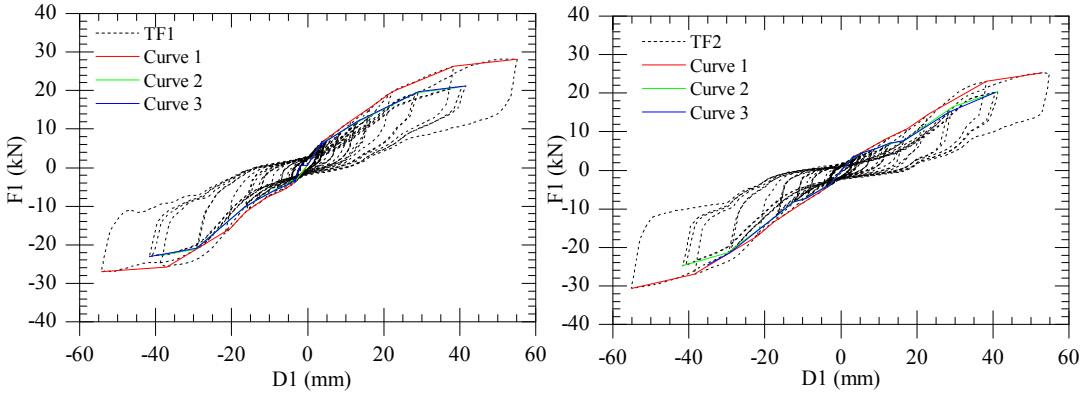

Fig.4 Load-displacement envelope curves

Properties such as stiffness, yield displacement, ductility and impairment of strength can be determined from the envelope curves according to the definitions adopted.

Stiffness may be calculated by equation 1 for the first, second and third envelope curves of the cyclic test specimens. Parameters $\nu_{40\%Fmax}$ and $\nu_{10\%Fmax}$ in equation (1) are the displacement values obtained at 40% and 10% of maximum load (Fmax), respectively, for the envelope curves.

$$K = \frac{0.3 \times F_{max}}{\upsilon_{40\%F_{max}} - \upsilon_{10\%F_{max}}} \quad (1)$$

Accordingly, based on the values presented in Table 1, the stiffness of the wall was estimated in 694 kN/m for TF1 specimen and in 526 kN/m for TF2 specimen (average of three curves). This difference could be related with the behaviour of timber connections and with the heterogeneity in material properties.

Table 1 Wall stiffness

TF1	F_{max} (kN)	F_{min} (kN)	$\lvert F_{ave}$ (kN)$\rvert$	$\nu_{40\%Fmax}$ (mm)	$\nu_{40\%Fmin}$ (mm)	$\nu_{40\%Fave}$ (mm)	$\nu_{10\%Fmax}$ (mm)	$\nu_{10\%Fmin}$ (mm)	$\nu_{10\%Fave}$ (mm)	K (kN/m)
1ª curve	28.2	-27.0	27.6	12.3	-15.4	13.9	1.1	-2.8	2.0	696.0
2ª curve	21.1	-22.8	21.9	8.7	-13.7	11.2	0.9	-2.8	1.9	703.6
3ª curve	21.3	-21.0	21.2	8.5	-13.7	11.1	0.9	-2.8	1.9	686.6
TF2	F_{max} (kN)	F_{min} (kN)	$\lvert F_{ave}$ (kN)$\rvert$	$\nu_{40\%Fmax}$ (mm)	$\nu_{40\%Fmin}$ (mm)	$\nu_{40\%Fave}$ (mm)	$\nu_{10\%Fmax}$ (mm)	$\nu_{10\%Fmin}$ (mm)	$\nu_{10\%Fave}$ (mm)	K (kN/m)
1ª curve	25.2	-30.7	27.9	18.2	-14.3	16.2	2.7	-1.7	2.2	598.2
2ª curve	20.3	-24.7	22.5	18.1	-13.5	15.8	2.3	-1.7	2.0	488.7
3ª curve	20.1	-24.6	22.4	18.0	-13.2	15.6	2.2	-1.7	2.0	492.5

The energy dissipated in each cycle may be evaluated by calculating the area within the load-displacement curve in each cycle. Fig. 5 and Table 2 show the behaviour of load - displacement of the walls along the cycles, where a decrease in damping with increasing imposed deformation can be observed. The damping coefficient for a given cycle may be estimated based on the following equation:

$$\zeta = \frac{E_d}{2\pi \times F_{max} \times d_{max}} \quad (2)$$

In equation (3), the dissipated energy, E_d, corresponds to the area of the graph delimited by the cycle, F_{max} is the maximum force measured on the structure during that cycle and d_{max} is the maximum deformation in the structure during that cycle.

The energy dissipation per cycle associated with the hysteretic behaviour of the wall was determined by measuring the area of the wider cycle in each stage of deformation in the force-displacement diagram. In Table 2 the energy dissipated in cycles at different levels of deformation is presented. The increase in deformation leads to a higher increase in energy dissipation and less damping, associated to damage in the wooden beams.

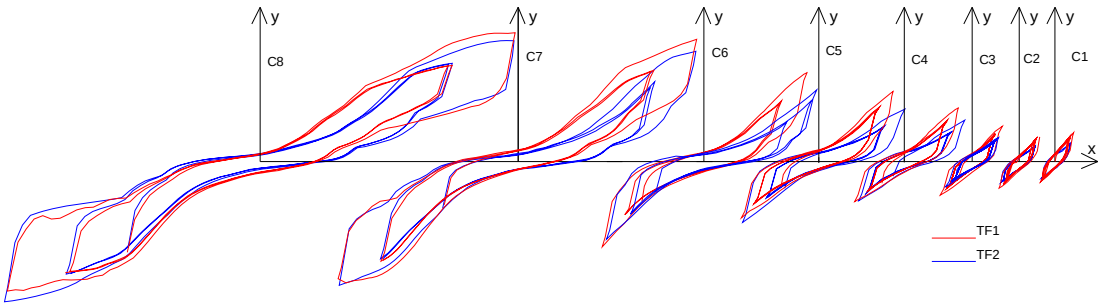

Fig.5 Energy dissipated in each cycle

Table 2 Energy dissipated and damping coefficient in each cycle

Cycle	TF1				TF2			
	$D_{max.(mm)}$	F_{max} (kN)	E_d.(kN/mm^2)	ζ (%)	$D_{max.(mm)}$	F_{max} (kN)	E_d.(kN/mm^2)	ζ (%)
C1	2,82	5,77	19,75	19	3,02	3,99	15,38	20
C2	4,54	7,18	26,35	13	4,63	4,22	17,70	14
C3	6,57	8,72	48,74	14	5,90	4,86	32,40	18
C4	11,30	12,14	111,03	13	11,91	8,18	99,90	16
C5	16,28	15,45	181,15	11	17,57	13,51	181,87	12
C6	22,26	19,76	270,68	10	23,23	14,65	253,25	12
C7	38,48	26,30	721,08	11	38,36	23,04	641,67	12
C8	55,24	28,21	1138,03	12	55,16	30,65	1071,00	10

The load was increasing with the imposed displacement until the rupture of one diagonal, which occurred, associated with lateral instability. Fig. 6 shows the failure modes of timber frames.

a) Failure by compression and lateral instability of diagonal in TF1

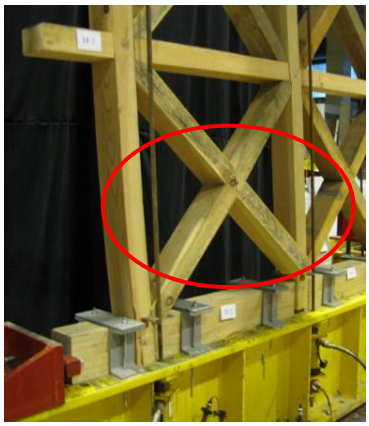

b) Failure by compression and lateral instability of diagonal in TF2

Fig.6 Failure mode of timber frames.

Masonry walls (MW)

Two masonry walls, MW1 and MW2, constituted by a timber frame with masonry infill, were submitted to the same displacement history as the timbre frames (TF).

Fig. 7 shows load-displacement diagrams, presenting an increase in the wall stiffness for displacements higher than 60 mm due to the increase of load in the jacks, as occurred in the TF specimens. Due to this behaviour, these values cannot be taken into account for the characterization of the walls and the analysis is limited to a range of ± 55 mm displacements, which results in a 2.6% drift. The maximum strength within this cycles' amplitude is 50 kN, measured at the displacement of 55 mm, corresponding to a significant drift of 2.6%.

The results presented on figure 7 show two distinct behaviours. In the first cycles the walls present practically linear behaviour, up to approximately 35 kN and 15 mm (0.7% drift). The small hysteresis loops in this phase are associated to gaps in the connections, which open and close according to the direction of the load. As displacement increases, a number of effects that characterize the nonlinear behaviour become visible around 45 kN load and 55 mm displacement which results in a 2.6% drift.

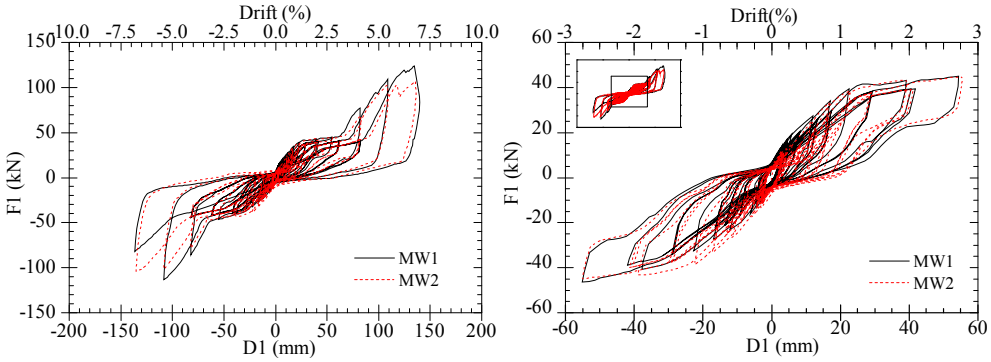

Fig.7 Force-displacement curves

A certain vertical lift of the bottom beam occurred during the wall test, as well as a separation of the vertical timber elements from the bottom beam, as an effect of a rocking movement that was not eliminated, becoming more significant with the increase of the overall deformation (Fig. 8).

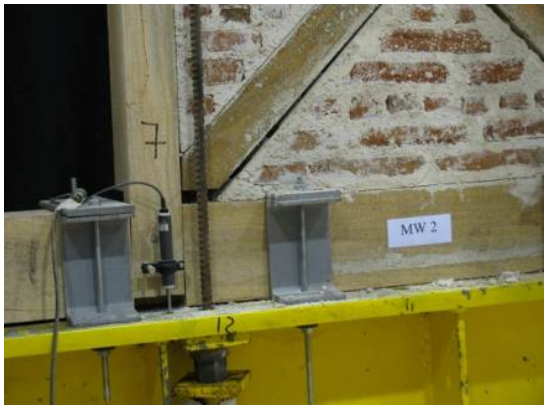

Fig. 8 Vertical lift of bottom beam and vertical member.

The curves shown in Fig. 9 correspond to the evolution of hysteretic behaviour of the walls MW1 and MW2 that showed an identical behaviour. According to ISO/DIS 21581, stiffness properties are determined by the envelope curves based on equation 1. Fig. 9 and Table 4 summarize the results need

to compute the walls stiffness, estimated in 2015 kN/m in the case of MW1 and 2000 kN/m in the case of MW2 (average of the three curves).

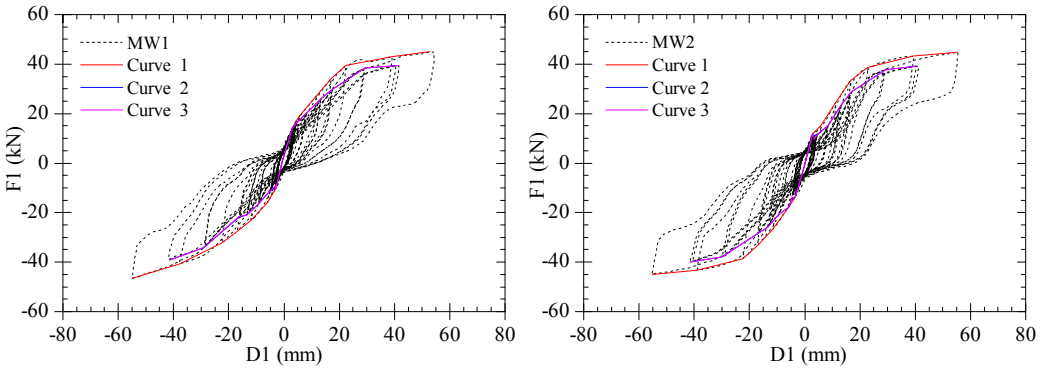

Fig. 9 Force-Displacement curves.

Table 4 Wall stiffness.

MW1	F_{max} (kN)	F_{min} (kN)	$\|F_{ave}$ (kN)$\|$	$\nu_{40\%} F_{max}$ (mm)	$\nu_{40\%} F_{min}$ (mm)	$\nu_{40\%}$ (mm)	$\nu_{10\%} F_{max}$ (mm)	$\nu_{10\%}$ F_{min}(mm)	$\nu_{10\%}F_{ave}$ (mm)	k (kN/m)
1ª curve	45.1	-55.0	50.1	6.1	-9.1	7.6	0.1	-1.5	0.8	2209.4
2ª curve	39.5	-41.5	40.5	4.5	-9.1	6.8	0.1	-1.5	0.8	2025.4
3ª curve	39.5	-41.5	40.5	4.5	-9.1	6.8	0.1	-1.5	0.8	2025.4
MW2	F_{max} (kN)	F_{min} (kN)	$\|F_{ave}$ (kN)$\|$	$\nu_{40\%} F_{max}$ (mm)	$\nu_{40\%} F_{min}$ (mm)	$\nu_{40\%}$ (mm)	$\nu_{10\%} F_{max}$ (mm)	$\nu_{10\%} F_{min}$ (mm)	$\nu_{10\%}F_{ave}$ (mm)	k (kN/m)
1ª curve	44.8	-55.1	49.9	9.2	-7.2	8.2	0.5	-1.0	0.8	2011.3
2ª curve	39.3	-41.3	40.3	8.7	-5.0	6.9	0.5	-1.0	0.8	1982.8
3ª curve	39.3	-41.3	40.3	8.7	-5.0	6.9	0.5	-1.0	0.8	1982.8

Fig. 10 shows the masonry walls hysteresis cycles along the test. According to equation 3 the damping coefficient in each cycle is obtained. In table 5 the energy dissipated in cycles at different levels of deformation is presented. The increase in deformation leads to an increase in energy dissipation and a decrease in damping, associated to damage in the timber beams and in the masonry infill.

When compared with the timber frames, the masonry walls present higher energy dissipation (about the double) and the some order of magnitude in damping coefficient.

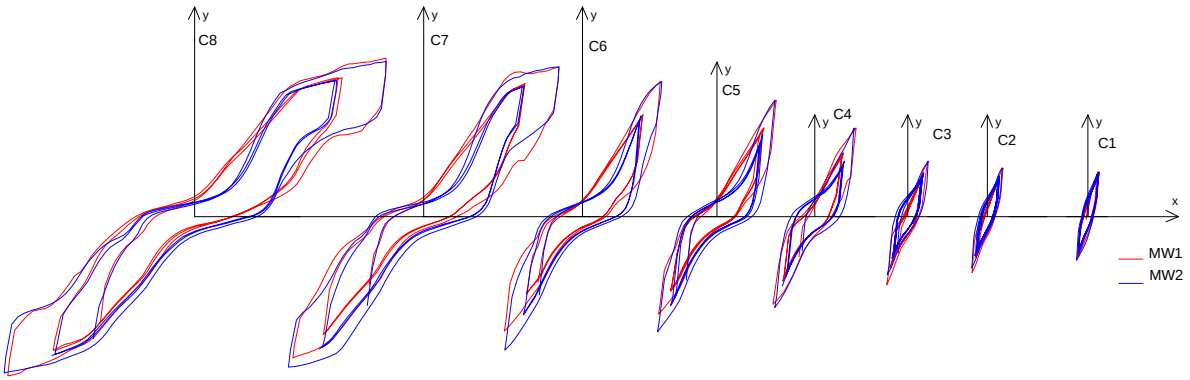

Fig. 10 Energy dissipated in each cycle

Table 5 Energy dissipated and damping in each cycle

Cycle	MW1				MW2			
	$D_{max.}$ (mm)	F_{max} (kN)	E.d(kN/mm^2)	ζ (%)	$D_{max.}$ (mm)	F_{max} (kN)	E.d(kN/mm^2)	ζ (%)
C1	3,3	13,88	48,29	16,9	3,28	13,65	58,45	20,7
C2	4,1	17,01	69,30	14,2	4,27	13,36	77,83	21,7
C3	6,14	16,21	97,74	15,6	5,93	17,76	114,59	17,3
C4	12,10	23,25	283,77	16,0	11,56	26,87	312,95	16,0
C5	17,11	34,14	416,15	11,3	17,22	33,40	483,28	13,4
C6	22,45	39,40	610,34	10,98	22,49	38,67	652,44	11,94
C7	39,18	43,06	1377,66	12,99	39,39	43,25	1406,89	13,14
C8	54,39	45,13	2043,75	13,25	55,12	44,99	1984,84	12,74

Fig. 11 shows the failure modes of the masonry walls. Rupture in MW1 is associated with compression of the diagonals that caused the shear failure of the intermediate beam. In the case of the model MW2 the wall had an early rupture by shear parallel of the timber fibres at one end of the intermediate beam.

a) Failure by shear of intermediate timber beam in MW1.

b) Failure by longitudinal shear of intermediate timber beam in MW2.

Fig. 11 Failure mode of masonry walls.

CONCLUSION

The load-displacement diagrams obtained for the timber frames (TF) and masonry walls (MW) are shown in Fig. 12. Through the analysis of the behaviour in the load-displacement diagrams, an increase in the wall stiffness for displacements higher than 60 mm was observed, associated with the course limit of the vertical jacks. Due to this behaviour, these values cannot be taken into account for the characterization of the walls. Therefore the analysis is limited to a range of ± 55 mm displacements as shown in Fig. 12.

The hysteretic behaviour of the timber framed wall subjected to cyclic loading is characterized by nonlinear behaviour, with a good ductility response. The maximum strength is 30 kN and 50 kN, for the timber frames and masonry walls respectively, measured at the displacement of 55 mm which results in a 2.6% drift.

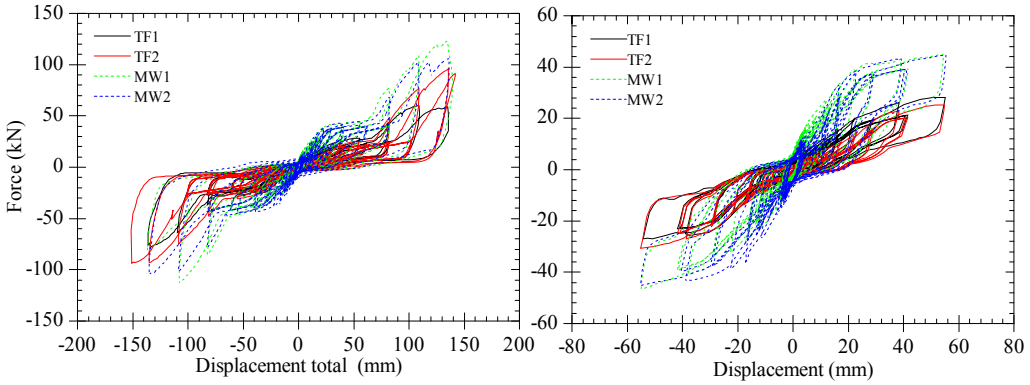

Fig. 12 Load-displacement diagrams.

As expected, masonry walls exhibited higher average stiffness than timber frames, of 2000 kN/m and 600kN/m respectively. Masonry infill proved to significantly influence the stiffness and especially the strength of the whole module. The masonry infill also influences the collapse mode, namely by preventing the lateral instability of the compressed diagonals.

The masonry walls also have a greater ability to dissipate energy, which implies a larger damping effect, a major relevance parameter regarding the behaviour of the walls subjected to earthquake loading.

NUMERICAL STUDY ON THE STRUTURAL BEHAVIOR OF POMBALINOS WALLS

Aiming at reproducing the experimental results, numerical finite element models were developed in ABAQUS. The models were calibrated based on the experimental results, assuming that, the diagonals of the wall are not able to work under tension (only compression); Links were used to simulate cross-halving joints in the connections between vertical and horizontal timber elements and between the crossing diagonals.

The boundary conditions are shown in Figure 13 a). The nodes affected by the boundary conditions have their displacements and rotations restrained and simulate the effect of the fixed beam connection on the base and lateral movement on the top. The models involved the application of horizontal and vertical load.

The mesh is composed by hexahedral elements with eight nodes each (element C3D8R from ABAQUS library) (Figure 13 b) and c)). The quality of the mesh is controlled by the user through the specification of several parameters, such as the aspect ratio of the elements, and is automatically generated through the top-down mesh generation algorithm available in the program.

The interaction properties between the different parts had to be defined in the assembled model. The assemblies are defined in two groups: the connector and interactions.

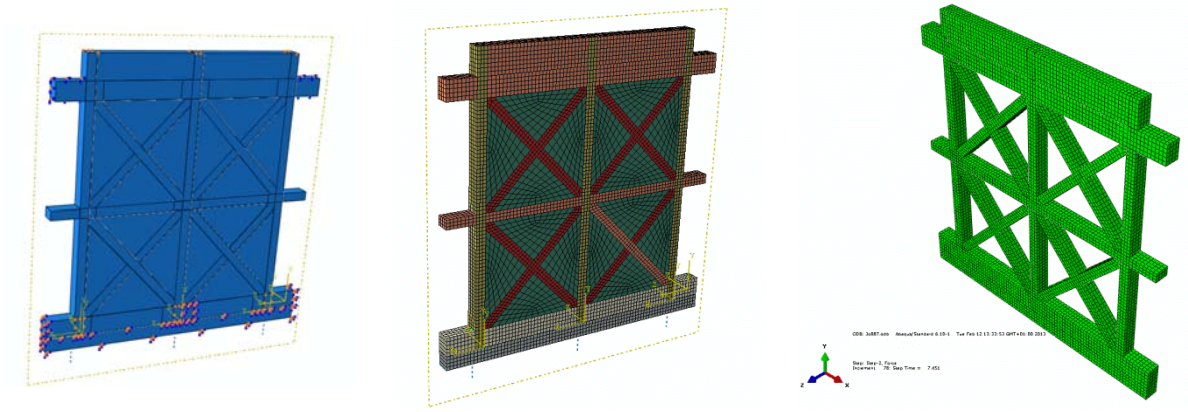

a) Boundary conditions b) Mesh of masonry walls c) Mesh of timber frames

Fig. 13 Numerical model

The relevant properties of pine wood used in the timber elements (Table 6) were obtained in Cruz *et al.* (1997). The masonry Poisson ratio ν is assumed to be 0.2 (Technical Tables, 1998). The mechanical properties of the materials "masonry" and "wood" are presented in Table 1.

Table 6 Materials properties

Characteristics of wood	Modulus of elasticity parallel to grain (GPa)	E_{mean}	12
	Shear modulus, mean (GPa)	G_{mean}	0.75
	Density, mean (kg/m3)	ρ_{mean}	580
	Density, characteristic value (kg/m3)	ρ_k	460
Characteristics of masonry	Modulus of elasticity (MPa)	$E_{masonry}$	770
	Density (kN/m^3)	$\rho_{masonry}$	22
	Poisson	ν	0.2

RESULTS

Fig. 14 shows the load-displacement curves of the model compared to experimental test results of timber frame wall TF2. As displacement increases a number of effects, such as cracking and plastification, lead to a decrease in stiffness, becoming more evident with the number of hysteretic cycles.

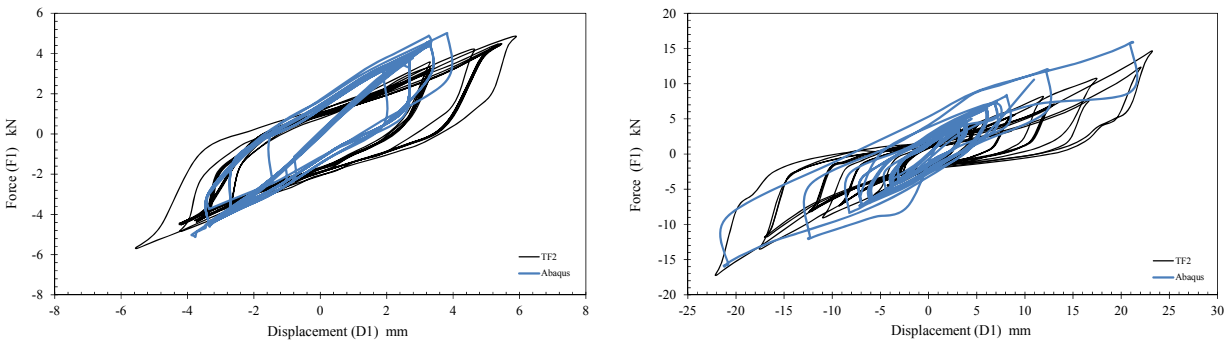

Fig. 14 Force-displacement curves of timber frames along the displacement history

Figure 14 shows the models deformed shape for a displacement of 5.4mm (left and right), with a scale factor of 50. It is observed that the stress is higher in vertical elements, as expected.

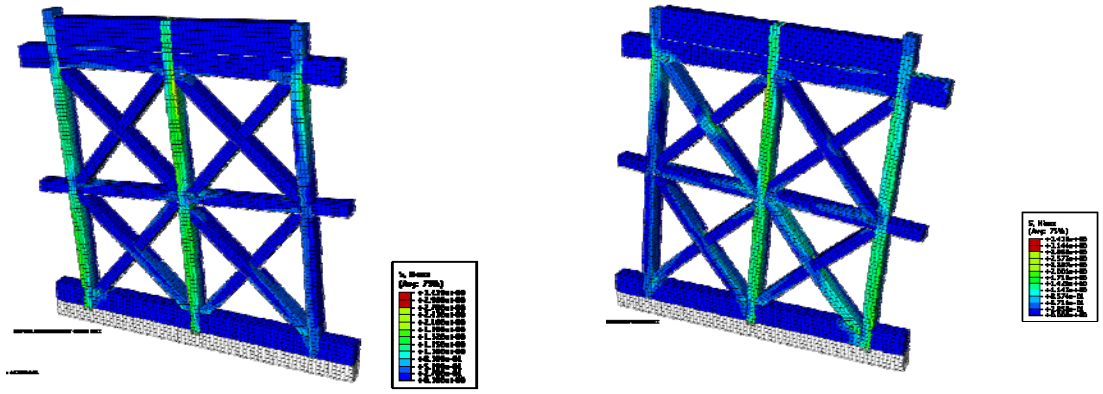

Fig. 14 Shear stress in the model, for a displacement of 5.4mm

CONCLUSION

The study developed in this paper showed that timber masonry walls are able to carry seismic loading with good resistance and deformation capacity, unlike ordinary masonry. Nevertheless, the strengthening with different methods, developed in this investigation, may improve the structural behaviour of these elements aiming obtaining an overall increase in the building response to earthquakes.

ACKNOWLEDGMENTS

The financial support of the Foundation for Science and Technology (FCT) through the research project PTDC/ECM/100168 – REABEPA is acknowledged. The authors also acknowledge HCI for his invaluable help. The laboratory technician Mr. Fernando Alves is also acknowledged for his help in the experimental tests.

REFERENCES

ASTM E2126 – 11. Standard Test Methods for Cyclic (Reversed) Load Test for Shear Resistance of Vertical Elements of the Lateral Force Resisting Systems for Buildings.

Diskaya, H. Damage Assessment of 19th Century Traditional Timber Framed Structures in Istanbul, From Material to Structure - Mechanical Behaviour and Failures of the Timber Structures, ICOMOS IWC - XVI International Symposium, November 2007.

Dogangun A., Tuluk I.O., Livaoglu R., Acar R. Traditional wooden buildings and their damages during earthquakes in Turkey. Engineering Failure Analysis (2006) 13, 981–996

Duţu A., Ferreira J., Guerreiro L., Branco F., Gonçalves A. Timbered masonry for earthquake resistance in Europe", Materiales de Construcción, 2012,Vol. 62, 308, 615 628, Out.-Dez.

EN 1991-1-1. Eurocode 1: Actions on structures –part 1-1: General actions – Densities, self-weight. Imposed loads for buildings, commissions of the European Communities (CEN), Brussels, April 2002.

Ferreira, J. G., Teixeira M.J., Dutu, A., Branco, F., Gonçalves, A., Experimental Evaluation and Numerical Modelling of Timber Framed Walls. Experimental Techniques, online since 27 March 2012.

Gonçalves A, Ferreira J., Guerreiro L, Branco F. Avaliação Experimental do Comportamento de Paredes de Edificios Pombalinos. Construlink ,2011,Vol. 9 : 27.

Gülkan, P., Langenbach, R. The earthquake resistance of traditional timber and masonry dwellings in Turkey. 13th World Conference on Earthquake Engineering Vancouver, 2004, B.C. No. 2297.

ISO 21581 (2010). Timber structures - Static and cyclic lateral load test methods for shear walls. New Delhi: Bureau of Indian Standards.

Krawinkler H., Parisi F., Ibarra L., Ayoub A. and Medina R. Development of a testing protocol for wood frame structures, Krawinkler. CUREE-Caltech Woodframe Project Rep., Stanford University, Stanford, California, 2000.

Langenbach, Randolph. From 'Opus Craticium' to the 'Chicago Frame': Earthquake-Resistant Traditional Construction. International Journal of Architectural Heritage, 2007 1: 1, 29 - 59.

Makarios, T., Demosthenous, M. Seismic response of traditional buildings of Lefkas Island, Greece. Engineering Structures, 2006, 28,264–278.

Meireles H.; Bento R. Cyclic Behaviour of Pombalino Frontal Walls. Proceedings of the 14th European Conference on Earthquake Engineering (14ECEE), 2010,Ohrid, F.Y.R.O. Macedonia.

Redondo, E. González, Hernández-Ros, R. Aroca. Wooden framed structures in Madrid domestic architecture of 17th to 19th centuries. Proceedings of the First International Congress on Construction History,2003, 20th-24th January .